Thin film growth and band lineup of In_2O_3 on the layered semiconductor InSe

O. Lang and C. Pettenkofer
Department of Physical Chemistry-Interfaces, Hahn-Meitner-Institute, D-14109 Berlin, Germany

J. F. Sánchez-Royo and A. Segura
Department of Applied Physics, University of Valencia, E-46100 València, Spain

A. Klein[a] and W. Jaegermann
Department of Materials Science, Darmstadt University of Technology, D-64287 Darmstadt, Germany

(Received 27 January 1999; accepted for publication 18 August 1999)

Thin films of the transparent conducting oxide In_2O_3 have been prepared in ultrahigh vacuum by reactive evaporation of indium. X-ray diffraction, optical, and electrical measurements were used to characterize properties of films deposited on transparent insulating mica substrates under variation of the oxygen pressure. Photoelectron spectroscopy was used to investigate *in situ* the interface formation between In_2O_3 and the layered semiconductor InSe. For thick In_2O_3 films a work function of $\varphi = 4.3$ eV and a surface Fermi level position of $E_F - E_V = 3.0$ eV is determined, giving an ionization potential $I_P = 7.3$ eV and an electron affinity $\chi = 3.7$ eV. The interface exhibits a type I band alignment with $\Delta E_V = 2.05$ eV, $\Delta E_C = 0.29$ eV, and an interface dipole of $\delta = -0.55$ eV.
 [S0021-8979(99)08322-X]

I. INTRODUCTION

In_2O_3 belongs to the class of transparent conducting oxides (TCOs) as SnO_2 or ZnO, which play an important role as window materials in optoelectronic devices.[1] The preparation of very efficient heterojunction solar cells is of particular interest for different absorber materials such as GaAs or InP[1–4] and thin film materials as, e.g., $CuInS_2$.[5] The main advantages of TCOs are their high transparency in the visible range (>90%), the good electrical conductivity ($\rho \leqslant 10^{-3}\,\Omega$ cm) as well as a high reflectivity in the infrared and a pronounced radiation resistance. The properties of In_2O_3 have been reviewed by Hamberg and Granqvist.[6]

In this paper we report on thin film growth of In_2O_3 on quartz glass and on the van der Waals surfaces of insulating mica and semiconducting InSe. Due to its direct band gap of $E_g = 1.26$ eV InSe is an interesting material for optoelectronic devices.[7] Interfaces between different layered materials epitaxially grown on each other exhibit only small interface dipoles due to the low density of interface states on van der Waals surfaces.[8–10] In contrast, large interface dipoles are observed at interfaces between layered compounds and three-dimensional heterocontact materials as found for CdS/InSe or CdS/WSe_2.[10] These dipoles originate from ''ionic dipoles'' related to the polar surface termination of the deposited 2–6 layer and are not associated with ''electronic dipoles'' related to active interface states.[10] This is confirmed by the fact that the highest efficiency (10.9%) for a solid state solar cell based on a layered semiconductor as absorber material has been achieved with the system indium–tin-oxide (ITO)/InSe/Au.[7,11,12] We have investigated the interface In_2O_3/InSe in more detail by surface sensitive techniques to better understand its properties in heterojunction solar cells.

The photovoltage V_{ph} generated in a heterojunction solar cell is affected by the band bending eV_{bb} in the absorber material and by the valence and conduction band offsets ΔE_V and ΔE_C, respectively. The determination of these values is hence of mutual interest. A schematic overview of the important parameters is given in Fig. 1. The values depicted for the work function φ, electron affinity χ, ionization energy I_P, and band gap E_g can be found in the literature for InSe[8,13] and for In_2O_3.[3,6,14–17] The wide scatter of the In_2O_3 values shows that more detailed experiments on In_2O_3 itself are needed. Therefore, as a first step, we have investigated In_2O_3 films prepared by reactive evaporation as a function of substrate temperature T_S and oxygen pressure p_{ox}. The films and their properties were characterized by standard x-ray diffraction, and by optical and electrical measurements. In addition x-ray and ultraviolet photoelectron spectroscopy (XPS, UPS) were applied to characterize the interface properties.

II. EXPERIMENT

The In_2O_3 films were deposited in a homemade ultrahigh vacuum (UHV) chamber equipped with an effusion cell for In evaporation, an O_2 gas inlet and a resistively heated manipulator allowing for sample temperatures ranging from 150 to 900 K. The distance between gas inlet aperture and the sample surface was about 15 mm. Deposition fluxes were controlled either by a quartz microbalance at the growth position or an ionization gauge. Both starting materials In and O_2 had a purity of 5 N each.

As substrates mica (muscovite) and arsenic doped *p*-InSe single crystals were used. The crystals were cleaved in air along the (0001) plane. Before film growth the sub-

[a]Author to whom correspondence should be addressed; electronic mail: aklein@hrzpub.tu-darmstadt.de

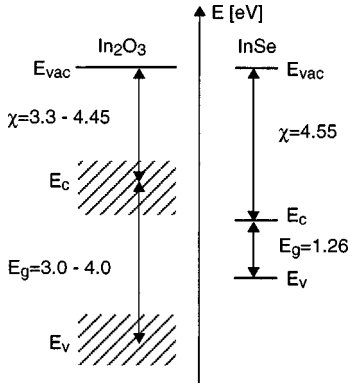

FIG. 1. Band model of the system In_2O_3/InSe before contact formation. The depicted range of values of band gap E_g, work function φ, electron affinity χ and ionization energy I_P is due to literature data from Refs. 3, and 14–17, and references therein. The values stated for InSe have been determined by Camassel *et al.* (Ref. 13) and by our group in previous experiments (Ref. 8).

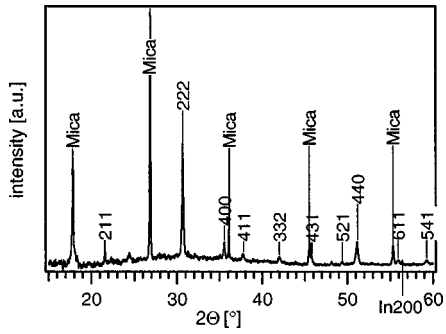

FIG. 2. X-ray diffraction pattern taken from a 240 Å In_2O_3 film prepared on a cleaved mica substrate at $T_S=250\,^{\circ}C$ and $p_{ox}=10^{-3}$ mbar. The mica labels refer to the (001) peaks of the mica (muscovite: JCPDS 6-263) substrate. Numbers indicate (*hkl*) values of the cubic In_2O_3 (JCPDS 6-416) phase. A small contribution of metallic indium is observed. The reflected intensity at $2\Theta=24.3°$ is attributed to the sample holder.

strates were annealed at $T_S=250-350\,^{\circ}C$ in order to remove remaining contaminations from the surface.

In situ characterization with UPS (He I and II) and XPS ($Mg\,K\alpha$) was performed in the attached UHV surface analysis system at a base pressure of 10^{-10} mbar. The energy resolution of UPS is below 100 meV, limited by the analyzer pass energy set to 6 eV. The energy resolution of XPS is limited by the linewidth of the unmonochromatized $Mg\,K\alpha$ excitation source. All spectra were taken in normal emission. After *in situ* characterization the films prepared on quartz glass and mica substrates were investigated in air with x-ray diffraction, optical absorption and Hall effect measurements. The optical transmission of the films was determined for wavelengths between 200 and 1700 nm. Film thicknesses were obtained from the interference fringe pattern in the transparent region of the optical transmission spectrum. The optical absorption coefficient has been calculated in the usual way from the transmission spectrum of the films. Room temperature Hall effect measurements were carried out in the van der Pauw configuration with a homebuilt experimental setup.

III. RESULTS AND DISCUSSION

A. Film growth, optical and electrical properties

The growth of reactively evaporated In_2O_3 films on GaAs and InP substrates under variation of substrate temperature and oxygen pressure has already been investigated in detail.[3,4,18] In these experiments the growth of polycrystalline films of the bcc In_2O_3 phase (C–rare earth structure) was found within a range of $T_S=100-330\,^{\circ}C$ and $p_{ox}=2-10\times10^{-4}$ mbar. A preferred (100) orientation and high phase purity was reported at $T_S=250\,^{\circ}C$ and $p_{ox}=5\times10^{-4}$ mbar. Therefore we selected a value of $T_S=250\,^{\circ}C$ for all film growth experiments and only varied the oxygen pressure p_{ox}. The need for the latter is due to the fact that the nominal p_{ox}, as measured in our configuration, should be lower compared to the actual pressure at the sample position due to the gas inlet configuration.

Figure 2 shows an x-ray diffraction pattern of an In_2O_3 film deposited on a mica (muscovite: JCPDS 6-263) substrate. The mica labels in Fig. 2 refer to the (001) peaks of the mica substrate. The film has been grown with $p_{ox}=1\times10^{-3}$ mbar and an In rate of 6–8 Å/min with a nominal thickness $d=240$ Å. Vertical lines with attached (*hkl*) numbers indicate expected peak positions of the cubic In_2O_3 phase (JCPDS 6-416) with $a_0=10-12$ Å.[19] The intensity at $2\Theta=24.3°$ cannot be explained by any *hkl* planes of mica, (cubic or hexagonal) In_2O_3, or metallic In. Compared to other reflections the peak at 24.3° exhibits a larger linewidth and might therefore be due to the sample holder.

Table I summarizes the results of Hall effect measurements performed at In_2O_3 films on electrically nonconducting mica substrates. The thicknesses of the films have been calculated from the interference fringe pattern in the transparent region of the spectra. Evidently, the films prepared at $p_{ox}=3\times10^{-4}$ and 6×10^{-4} mbar exhibit the highest carrier concentration n, the lowest resistivity ρ and moderate values of the electron mobility μ.

Figure 3 shows the absorption coefficient obtained from the optical transmission spectrum of the In_2O_3 films on mica prepared at different oxygen pressures. The band gaps of the films are evaluated by linear extrapolation of the square of the absorption coefficient. The results are also given in Table I. The fact that the band gap increases with carrier concentration suggests that a widening of the optical gap occurs due to a partial filling of the conduction band (Burstein–Moss shift).[20,21] The optical gap is given within the Burstein–Moss theory by the relation:

$$E_g=E_{g0}+\frac{\hbar^2}{2m^*}\cdot(3\pi^2 n)^{2/3}, \tag{1}$$

TABLE I. Values of carrier concentration n, resistivity ρ and electron mobility μ of In_2O_3 films prepared on mica.

p_{ox} (mbar)	n (10^{19} cm^{-3})	μ (cm^2/V s)	ρ (10^{-3} Ω cm)	E_g (eV)	d (nm)
1×10^{-4}	2.2	46	6	3.55	30
3×10^{-4}	5.4	52	2.2	3.71	47
6×10^{-4}	7	36	2.5	3.8	33
1×10^{-3}	5.6	40	2.9	3.77	73

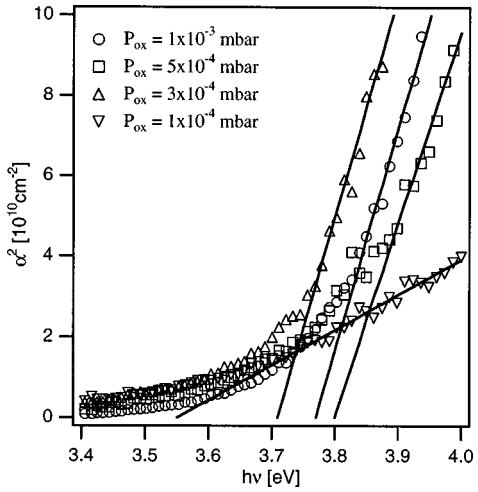

FIG. 3. Square of the optical absorption coefficient as a function of photon energy of different In_2O_3 films prepared on a cleaved mica (0001) substrate at $T_S = 250\,^{\circ}C$.

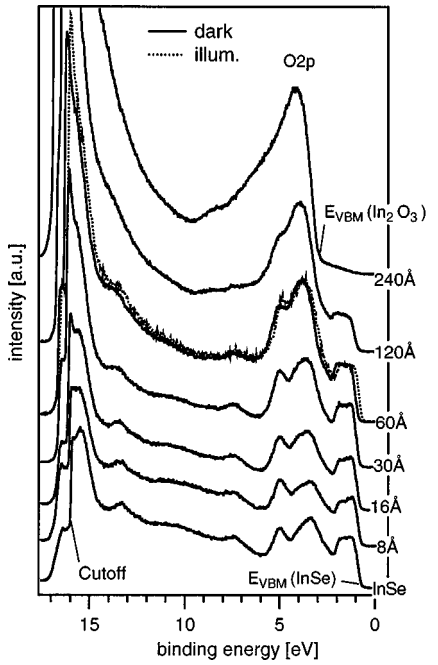

FIG. 4. Valence band photoelectron spectra (He I excitation) from In_2O_3 films stepwise deposited on InSe at $T_S = 250\,^{\circ}C$ and $p_{ox} = 5 \times 10^{-4}$ mbar. The binding energy positions of the valence band maximum and the secondary electron cutoff are indicated for the substrate spectrum.

where E_{g0} is the band gap of the undoped semiconductor, m^* is the reduced effective mass of the electrons and holes and n is the free electron concentration. Assuming $m^* = 0.6m_0$ (m_0 is the free electron mass),[6,22] and inserting values for n from Table I, we calculated an E_{g0} for each film. The average band gap for our In_2O_3 films finally is $E_{g0} = 3.63$ eV, which agrees well with literature data.[6,16]

B. In_2O_3/InSe interface formation

For the investigation of interface properties and band lineup between In_2O_3 and InSe we used the optimized deposition parameters for the preparation of well ordered and highly conductive In_2O_3 films assuming a similar growth behavior on InSe substrates as on mica. Thus stepwise film deposition was performed at $T_S = 250\,^{\circ}C$, $R_{In} = 8$ Å/min and $p_{ox} = 5 \times 10^{-4}$ mbar.

The growth mode of In_2O_3 on the cleaved InSe (0001) surface can be deduced from film and substrate intensities in the photoemission experiments. The He I valence band spectra presented in Fig. 4 show a clear contribution of In_2O_3 emissions only for nominal coverages of 60 Å and more. This significantly exceeds the surface sensitivity of the technique (10–20Å) and therefore indicates island growth which is supported by the XPS core level intensities. Island (Vollmer–Weber) growth is typically observed for metals on van der Waals surfaces[23] and also governs the growth of 2–6 semiconductors on layered materials.[24,25] It can be explained by the small surface free energy of the van der Waals planes and the small interface energy for nonreactive adsorbates, which does not favor surface wetting. The high surface free energy for three-dimensional materials as In_2O_3 therefore leads to the formation of three-dimensional islands during film growth. In contrast, the growth of layered materials on each other proceeds in a more pronounced layer-by-layer (Frank–van der Merwe) growth mode.[26] In comparison, growth of In_2O_3 films on Si(111) is described by a Stranski–Krastanov mode with a two-dimensional wetting layer followed by three-dimensional island growth.[27]

The valence band spectra of the InSe substrate with increasing In_2O_3 film thickness (Fig. 4) show a strong asymmetric emission between 2.75 and 9.5 eV binding energy originating from the In_2O_3 valence bands which are mostly derived from O $2p$ states. The measured valence band spectrum is in close agreement to published spectra.[27,28] For intermediate coverages the spectra can be described as a superposition of InSe substrate—and In_2O_3 film—emissions. Emissions from the InSe valence band can still be identified at a nominal film thickness of 120Å further establishing the three-dimensional growth mode of the In_2O_3 film.

Interface properties can be deduced from spectra of the In $4d$ core level taken with high resolution (He II excitation) shown in Fig. 5. Besides a small binding energy shift of about 150 meV no change in shape or linewidth, which would indicate an interface reaction or interdiffusion, is detected until $d = 60$ Å. At $d = 120$ Å the In $4d$ line is broadened due to a higher amount of In_2O_3 islands on the substrate surface. For the highest coverage a broad In $4d$ line has evolved, which is characteristic for stoichiometric In_2O_3.[28]

The band lineup can be determined from the binding energies of the valence band maxima of substrate E_V^s and film E_V^f, as a function of coverage. The result is shown in Fig. 6. To obtain the valence band maximum position of the In_2O_3 film (E_V^f) difference spectra were calculated for coverages of 60 and 120 Å, respectively: the spectrum of cleaved InSe was shifted in binding energy by the respective band bending qV_{bb} obtained from core-level shifts, multiplied by a suitable factor and finally subtracted from the spectrum. The obtained difference spectra resemble the spectrum obtained for the highest In_2O_3 coverage. The valence band offset ΔE_V is evaluated using the equation

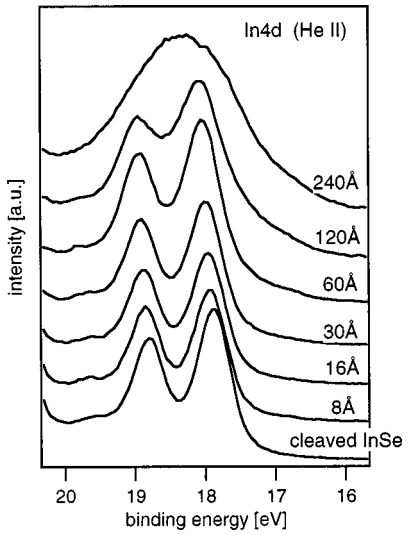

FIG. 5. UP spectra of the In 4*d* core-level excited with He II excitation from In_2O_3 films stepwise deposited on InSe.

$$\Delta E_V = E_V^f - E_V^s - qV_{bb}. \tag{2}$$

The conduction band offset ΔE_C is obtained by

$$\Delta E_C = \Delta E_g - \Delta E_V, \tag{3}$$

where ΔE_g is the difference in band gap for substrate and film material.

From the diagram given in Fig. 6, the values of E_V^f, E_V^s and qV_{bb} are 2.98, 0.70 and 0.23 eV, respectively, with estimated uncertainties of ± 0.1 eV each. We hence obtain $\Delta E_V = 2.05(\pm 0.15)$ eV and $\Delta E_C = 0.29(\pm 0.2)$ eV. The larger uncertainty in ΔE_C is due to additional uncertainties from the band gaps. The resulting band diagram of the system In_2O_3/InSe is presented in Fig. 7.

The work function φ of the sample, as obtained from the secondary electron cutoff of He I excited valence band spectra, shows a discontinuity δ at the interface which is deduced from the relation

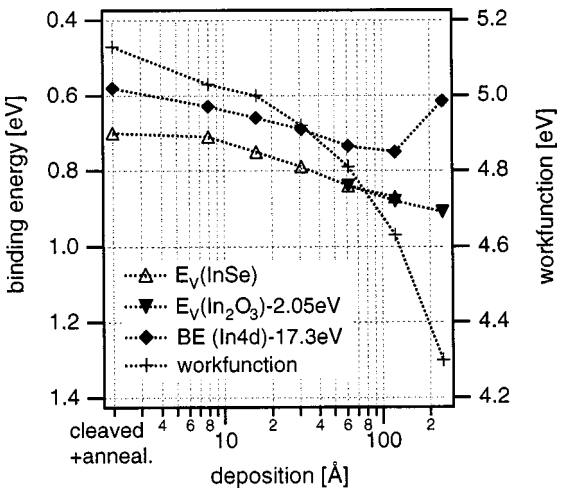

FIG. 6. Values of In 4*d* binding energy, valence band maximum and work function obtained from UPS measurements (see Figs. 4 and 5).

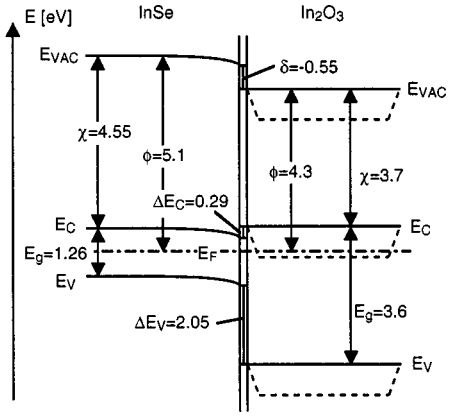

FIG. 7. Band diagram of the system In_2O_3/InSe in contact as determined from the present experiment. All values are in eV. With the common assumption of degenerately doped bulk In_2O_3 in conjunction with a surface depletion layer, the course of the band edges would be as indicated by the dashed lines.

$$\delta = I_P(In_2O_3) - I_P(InSe) - \Delta E_V. \tag{4}$$

Therefore the strong rise of the measured work function from $d = 30-240$ Å corresponds to an interface dipole $\delta = -0.55$ eV. For an unreacted interface region this interface dipole can be assumed to have a structural origin as also suggested for the system CdS/InSe.[10,29] In the latter case the dipole was determined as $\delta = +0.5$ eV and assigned to the difference of the ionization potential between the polar (0001) and $(000\bar{1})$ surface of CdS and the tendency of 2–6 compound films to grow with their cationic (0001) surfaces on top of the hexagonal van der Waals surface. For the In_2O_3/InSe interface an alternating electrostatic potential in the growth direction would be due to the polar In–O bond. The direction of the interface dipole, which is opposite to the CdS/InSe interface, indicates that the termination of the In_2O_3 film towards the InSe surface is anionic (oxygen termination; see also discussion below).

The experimentally determined position of the Fermi level of the In_2O_3 film, which is less than 3 eV above the valence band maximum, indicates a distance to the conduction band minimum of $E_C - E_F > 0.6$ eV for a band gap of 3.6 eV. This particular Fermi level position obtained for reactively evaporated In_2O_3 films by *in situ* photoelectron spectroscopy is consistent with independently determined values.[16,28,30] It is, however, in contradiction to the common assumption that transparent conductive oxides are degenerate *n*-type semiconductors (see, e.g., Ref. 6), which would give a Fermi level position inside the conduction band $E_C - E_F < 0$ eV or $E_F - E_V \geqslant 3.6$ eV. The electrical and optical data of our films deposited on mica substrate agree with this standard model. But, in none of our photoemission studies have we observed a value for $E_F - E_V$ in excess of 3.1 eV, even for films which clearly show a large number of defect states in the band gap region.[28] A Fermi level position of $E_F - E_V = 2.6$ eV determined by UPS has been explained by Cox *et al.*[30] with an indirect gap of In_2O_3 at this energy. Although such an indirect gap is frequently mentioned in the literature (see, e.g., Refs. 6, 30, and 31) it is not well established. The Burstein–Moss effect for the direct gap at $E_{g,dir} = 3.6$ eV in-

dicates that $E_F - E_V \geqslant 3.6\,\text{eV}$. With $E_{g,\text{ind}} = 2.6\,\text{eV}$ the Fermi level would lie more than 1 eV above the bottom of the corresponding conduction band. As a consequence the high concentration of free carriers would result in metallic conduction and an opaque material.

Comparable results were reported for SnO_2 surfaces, where the Fermi level is also observed well below the conduction band minimum which has been explained by a surface depletion layer.[32,33] A surface depletion layer could be introduced by oxygen adsorbed on the surface,[34] which is likely to occur during our film preparation involving a high oxygen pressure.

The presence of a surface depletion layer would explain the high doping and the large optical gap of our films (bulk properties) as well as the position of the surface Fermi level inside the band gap. However, since the doping of the films is rather high (see Table I), the surface space charge layer should extend only over a few nanometers. By lowering the surface sensitivity of UPS, which is possible with the variable photon energies from a synchrotron storage ring, there should be an observable movement of the valence band maximum to higher binding energies. So far we could not detect any shift of the valence band maximum from such studies. Therefore we cannot draw any conclusions on the existence of a depletion layer at the In_2O_3 surface. More detailed studies of the electronic defect structure of In_2O_3 and its different surfaces would be necessary to resolve this point.

The experimentally determined values for the band lineup of $\Delta E_V = 2.05\,\text{eV}$ and $\Delta E_C = 0.29\,\text{eV}$ may explain the reasonably good performance of the n^+-In_2O_3/p-InSe device structure with respect to applications such as solar cells or photodetectors. First, there is a large barrier ΔE_V for the transport of holes as majority carriers from the InSe absorber into the In_2O_3 window material. Second, the contact between the InSe conduction band and In_2O_3 does not hinder the transport of electrons photogenerated in the InSe absorber across the junction. In addition it can be expected that for higher doped p-InSe (about $10^{17}\,\text{cm}^{-3}$) a band bending of about 0.8 eV can be achieved which may lead to photovoltages of about 0.4–0.6 eV.

IV. SUMMARY AND CONCLUSION

Highly conductive films of In_2O_3 have been prepared by reactive evaporation of indium in oxygen atmosphere on the layered materials mica and InSe. Structural, optical and electrical properties of the films and of their interface with the semiconductor InSe were investigated. The films exhibit low electrical resistivities down to $\rho = 2 \times 10^{-3}\,\Omega\,\text{cm}$. We have determined the band gap ($E_{g0} = 3.6\,\text{eV}$), work function ($\varphi = 4.3\,\text{eV}$) and difference between the Fermi level and the valence band maximum ($E_F - E_V = 3.0\,\text{eV}$) for the In_2O_3 film. These values result in an electron affinity of $\chi = 3.7\,\text{eV}$ and an ionization energy of $I_P = 7.3\,\text{eV}$.

The grown In_2O_3/InSe junction reveals no reacted interface layer. The band lineup has been determined [$\Delta E_V = 2.05(\pm 0.15)\,\text{eV}$, $\Delta E_C = 0.29(\pm 0.2)\,\text{eV}$] and exhibits an overall interface dipole of $\delta = 0.55\,\text{eV}$ that is attributed to structural effects within the oxide layer by a polar interface termination. However, the band alignment of the system In_2O_3/InSe suggest that it may be an encouraging system for optoelectronic applications.

[1] T. J. Coutts and S. Nassem, Appl. Phys. Lett. **46**, 164 (1985).
[2] K. Ito and T. Nakazawa, J. Appl. Phys. **58**, 2638 (1985).
[3] V. Korobov, M. Leibovitch, and Y. Shapira, J. Appl. Phys. **74**, 3251 (1993).
[4] V. Korobov, Y. Shapira, S. Ber, K. Faleev, and D. Zushinskiy, J. Appl. Phys. **75**, 2264 (1994).
[5] Y. Ogawa, A. Jäger-Waldau, Y. Hashimoto, and K. Ito, Jpn. J. Appl. Phys., Part 2 **33**, L1775 (1994).
[6] I. Hamberg and C. G. Granqvist, J. Appl. Phys. **60**, R123 (1986).
[7] A. Segura, J. P. Guesdon, J. M. Besson, and A. Chevy, J. Appl. Phys. **54**, 876 (1983).
[8] O. Lang, A. Klein, C. Pettenkofer, W. Jaegermann, and A. Chevy, J. Appl. Phys. **80**, 3817 (1996).
[9] R. Schlaf, O. Lang, C. Pettenkofer, W. Jaegermann, and N. R. Armstrong, J. Vac. Sci. Technol. A **15**, 1365 (1997).
[10] R. Schlaf, T. Löher, O. Lang, A. Klein, C. Pettenkofer, and W. Jaegermann, Mater. Res. Soc. Symp. Proc. **448**, 469 (1997).
[11] A. Segura, M. C. Martinez-Tomás, B. Marí, A. Casanovas, and A. Chevy, Appl. Phys. A: Mater. Sci. Process. **44**, 249 (1987).
[12] A. Segura, J. P. Martinez, J. L. Valdes, F. Pomer, and A. Chevy, *Proceedings of the 7th European Photovoltaic Solar Energy Conference* (Reidel, Dordrecht, 1987), p. 475.
[13] J. Camassel, P. Merle, H. Mathieu, and A. Chevy, Phys. Rev. B **17**, 4718 (1978).
[14] E. Wang and L. Hsu, J. Electrochem. Soc. **125**, 1328 (1978).
[15] A. Myszkowski, L. Sansores, and J. Tagüena-Martinez, J. Appl. Phys. **52**, 4288 (1981).
[16] H. Öfner, Y. Shapira, and F. P. Netzer, J. Appl. Phys. **76**, 1196 (1994).
[17] Y. Park, V. Choong, Y. Gao, B. R. Hsieh, and C. W. Tang, Appl. Phys. Lett. **68**, 2699 (1996).
[18] A. Golan, Y. Shapira, and M. Eizenberg, J. Appl. Phys. **72**, 925 (1992).
[19] M. Marezio, Acta Crystallogr. **20**, 723 (1966).
[20] E. Burstein, Phys. Rev. **93**, 632 (1954).
[21] T. S. Moss, Proc. Phys. Soc. London, Sect. B **67**, 775 (1954).
[22] P. Manivannan and A. Subrahmanyam, J. Phys. D **26**, 1510 (1993).
[23] W. Jaegermann, C. Pettenkofer, and B. A. Parkinson, Phys. Rev. B **42**, 7487 (1990).
[24] T. Löher, Y. Tomm, C. Pettenkofer, and W. Jaegermann, Appl. Phys. Lett. **65**, 555 (1994).
[25] T. Löher, Y. Tomm, A. Klein, D. Su, C. Pettenkofer, and W. Jaegermann, J. Appl. Phys. **80**, 5718 (1996).
[26] O. Lang, R. Schlaf, Y. Tomm, C. Pettenkofer, and W. Jaegermann, J. Appl. Phys. **75**, 7805 (1994).
[27] H. Öfner, J. Kraft, S. L. Hofmann, S. L. Surnev, F. P. Netzer, J. Paggel, and K. Horn, Surf. Sci. **316**, 112 (1994).
[28] A. Klein, O. Henrion, C. Pettenkofer, W. Jaegermann, N. Ashkenasy, B. Mishori, and Y. Shapira, *Proceedings of the 14th European Photovoltaic Solar Energy Conference* (H.S. Stephens, Bedford, 1997), p. 1705.
[29] T. Löher, A. Klein, Y. Tomm, C. Pettenkofer, and W. Jaegermann, Semicond. Sci. Technol. (submitted for publication).
[30] P. A. Cox, W. R. Flavell, and R. G. Egdell, J. Solid State Chem. **68**, 340 (1987).
[31] R. L. Weiher and R. P. Ley, J. Appl. Phys. **37**, 299 (1966).
[32] D. F. Cox, T. B. Fryberger, and S. Semancik, Phys. Rev. B **38**, 2072 (1988).
[33] R. Cavicchi, M. Tarlov, and S. Semancik, J. Vac. Sci. Technol. A **8**, 2347 (1990).
[34] V. E. Henrich and P. A. Cox, *The Surface Science of Metal Oxides* (Cambridge University Press, Cambridge, 1994).